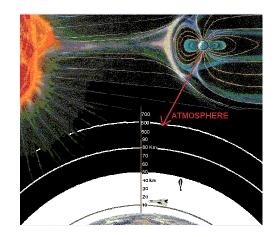
Modelling the outer radiation belt as a complex system in a self-organised critical state

Norma B. Crosby

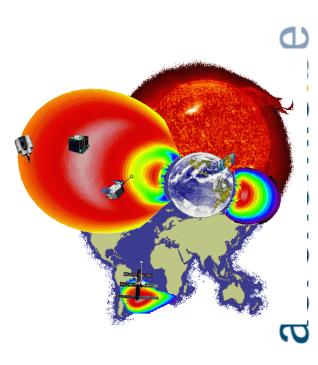
Belgian Institute for Space Aeronomy Ringlaan-3-Avenue Circulaire, 1180 Brussels, Belgium







When a method has been applied successfully on one part of the Sun-Earth Scenario (e.g. solar corona) one can investigate if it can also be applied successfully on another part (e.g. Earth's magnetosphere).



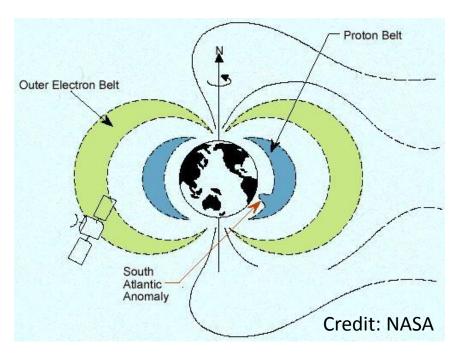
FREQUENCY DISTRIBUTIONS FREQUENCY DISTRIBUTIONS

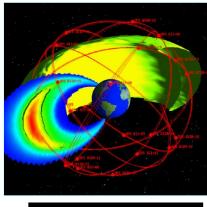




EARTH'S RADIATION BELTS

Trapped particle populations





Courtesy of U.S. Air Force Phillips Laboratory

Proton Belt: 1.3 R_E

Electron Inner Belt: 1.5 - 2.5 R_E Electron Outer Belt: 3-9 R_E

Protons: Tens keV – couple of hundreds of MeV

Electrons: Tens keV – several MeV



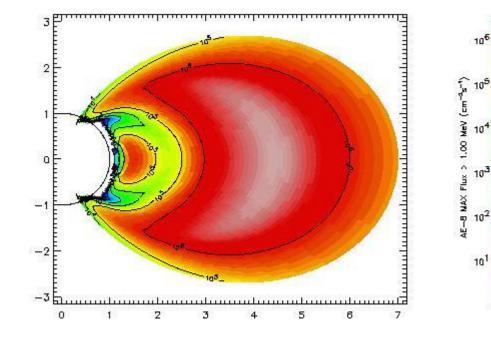
aeronomie.be

EARTH'S ELECTRON RADIATION BELTS

from STATIC MODELS to Dynamic Behaviour (on all spatial- and time-scales)

L-shell, L-value, or McIlwain Lparameter (McIlwain, 1961):

Motions of low-energy charged particles in the Earth's magnetic field can be usefully described in terms of McIllwain's (B,L) coordinates [B: magnitude (or length) of the magnetic field vector].



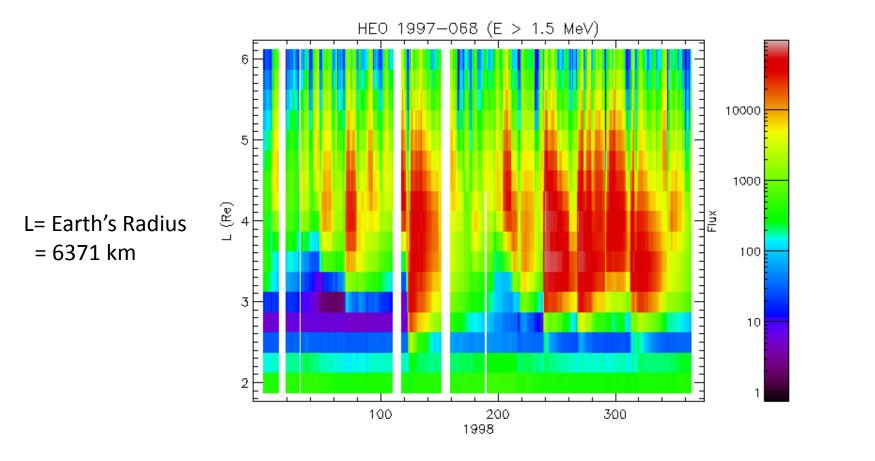
Invariant coordinate map of the AE-8 MAX integral electron flux >1 MeV. The semi-circle represents the surface of the Earth, distances are expressed in Earth radii.

Courtesy of SPENVIS (http://www.spenvis.oma.be/)



aeronom

Outer electron radiation belt is highly variable. \checkmark



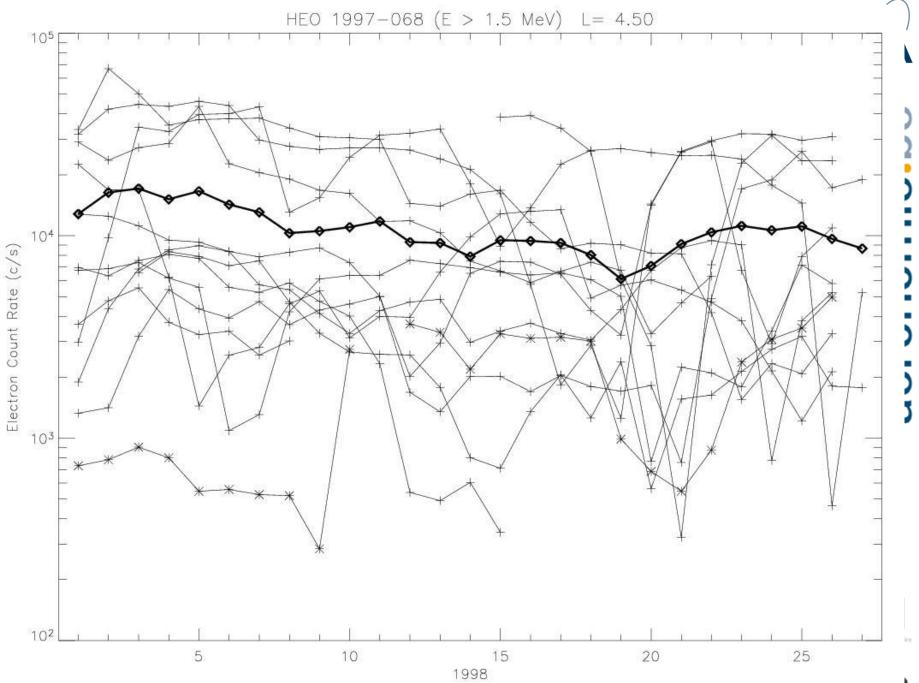
Daily Averaged Electron Outer Radiation Belt Count Rate Data



aeronomie.

HEO data courtesy of The Aerospace Corporation





Theories of electron acceleration include shock acceleration, classical radial diffusion, ULF enhanced radial diffusion, large- and small-scale recirculation, direct substorm injection, and Landau and cyclotron res

Any successful model should be able to explain

)06

on

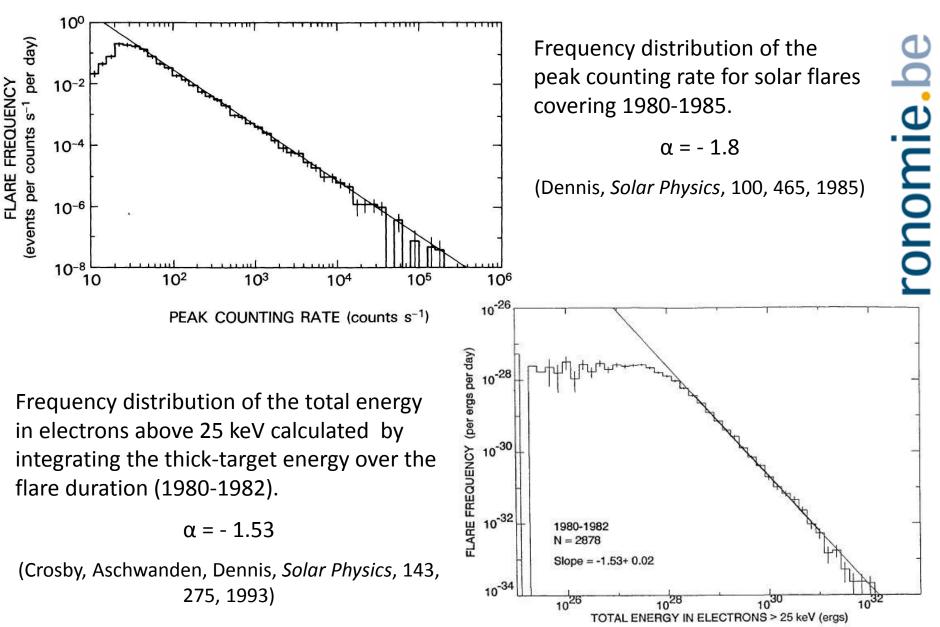
Ke [or at least to reproduce]

the results of statistical studies up(performed on the data.

datuvuse unu LANI-GLO yeusynunuuus suuennes.

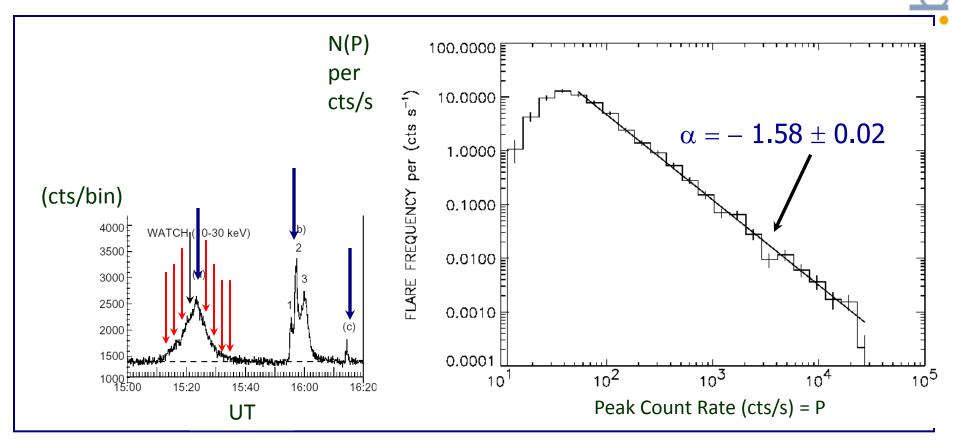
"The findings support a model whereby solar wind velocity drives convective transport of source and seed electrons, to the inner magnetosphere, where local acceleration and subsequent radial diffusion is responsible for the enhanced fluxes."

SOLAR FLARES [HXRBS/SMM]



SOLAR FLARES [WATCH/GRANAT]

1990, April-Dec.1991, Jan.-April, July 1992



Crosby N., Vilmer N., Lund N., Sunyaev R., Astron. Astrophys., 334, 299, 1998





THE ANALOGY – PART 1

DO

aeronomie.

Count rate frequency distribution of more than 5000 hard X-ray structures (less than 1 s) detected in 640 solar flares was found to be well-represented by a power-law with a slope of -1.84 (Aschwanden et al., 1995).

This is identical with what was found for the global frequency distribution behaviour of solar flare hard X-rays (e.g. Dennis, 1985; Crosby et al., 1993).

From a scale-invariant model like the avalanche model one would expect that the individual pulses that make up an "avalanche" would also show power-law behaviour and that the slope values would be similar.

THE ANALOGY – PART 2

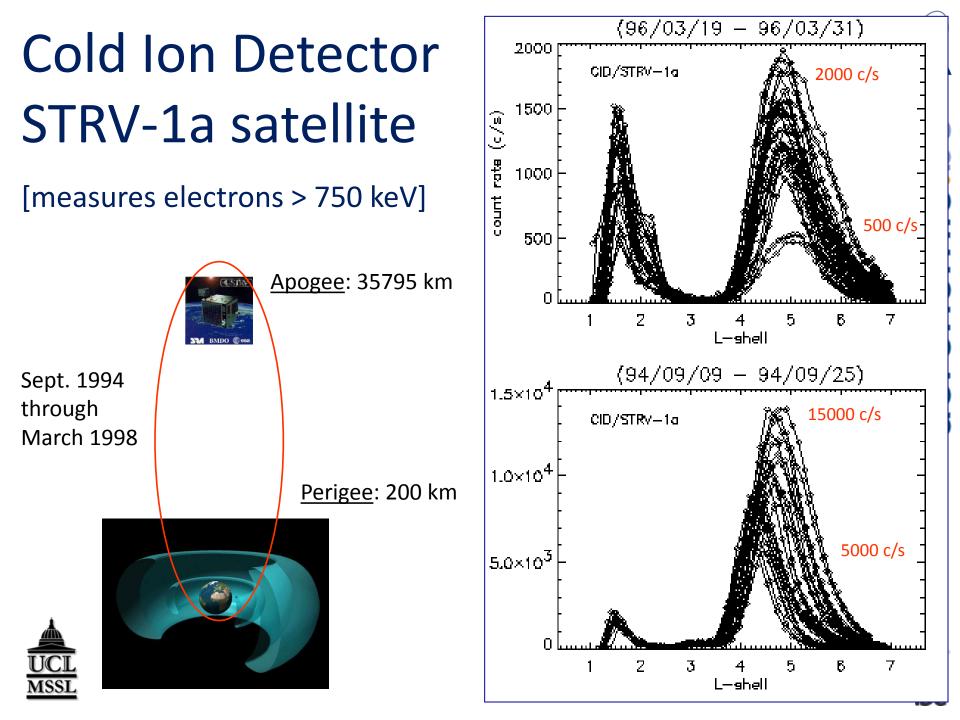


Even though there are no individually defined "avalanches" in the outer radiation belt, as there are, for example, in the case of the solar corona (e.g. solar flares), one can imagine that the outer radiation belt acts as one individual system "one flare".

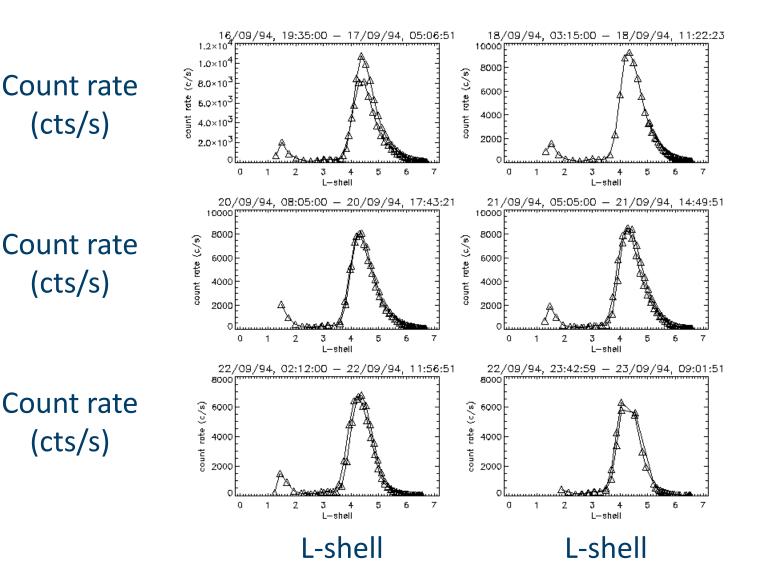
The analogy is that the pulses that make up the outer radiation belt are identical with the burst structures making up a flare "individual avalanche".

Bearing this in mind and the fact that the outer electron radiation belt is indeed dynamical on all spatial and temporal scales, one can speculate if perhaps the outer electron radiation belt also exhibits power-law behavior and thus exibiting itself as a candidate for SOC behaviour.





CID/STRV-1a (individual orbit plots)



(cts/s)

(cts/s)

(cts/s)

aeronomie.b



Crosby N., Meredith N., Coates A., Iles R., NPG, 12, 993, 2005

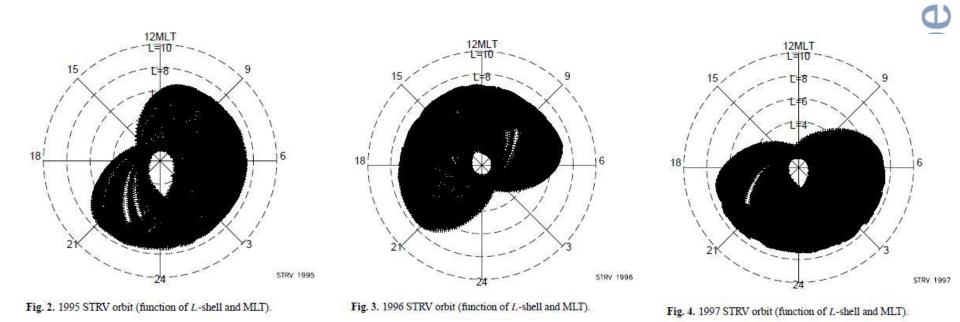


Table 2. Characteristics of the electron count rate (CR) frequency distributions for different MLT intervals for 1995–1997.

MLT	4.1-7.7	4.1-7.7	4.4-5.5	4.1-5.5	5.5-7.7	5.5-7.7	
	interval	slope	interval	slope	interval	slope	
0-6	[60,12079]	-1.674±0.007	[150,12079]	-1.517±0.015	[60,7609]	-1.959±0.015	1
6-12	[60,11837]	-1.522 ± 0.007	[150,11837]	-1.319 ± 0.014	[60,5345]	-1.705 ± 0.010	:
12-18	[60,9500]	-1.540 ± 0.010	[150,9500]	-1.476±0.019	[60,4456]	-1.824 ± 0.018	,
18-24	[60,8611]	-1.803 ± 0.010	[150,7815]	-1.819 ± 0.019	[60,8611]	-2.234 ± 0.017	



.be

OUTER ELECTRON RADIATION BELT



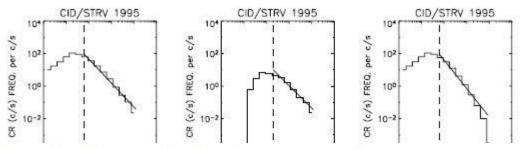


Table 1. Characteristics of the electron count rate (CR) frequency distributions for different years and L-shell intervals.

Year	4.1–7.7 interval	4.1-7.7 slope	4.1–5.5 interval	4.1-5.5 slope	5.5–7.7 interval	5.5–7.7 slope
1995–1997	[60,12079]	-1.634±0.004	[200,12079]	-1.602 ± 0.009	[60,8611]	-1.911 ± 0.006
1995	[60,12079]	-1.476 ± 0.007	[200,12079]	-1.373 ± 0.015	[60,8611]	-1.749 ± 0.011
1996	[60,9500]	-1.655 ± 0.006	[200,9500]	-1.589 ± 0.016	[60,4456]	-1.856 ± 0.010
1997	[60,8842]	-1.728 ± 0.008	[200,8842]	-1.786 ± 0.018	[60,4662]	-2.100 ± 0.014
10 ² - 10 ²	A A A	10° 10° 10° 10° 10° 10° 10° 10°		10^{0}		v N., Meredith N A., Iles R., NPG, 993, 2005
100						
C	$\frac{10^{1}}{R} \frac{10^{2}}{(c/s)} \frac{10^{2}}{for} \frac{10^{3}}{L=[4,1-7,7]}$ R (cts/s) fo = [4.1-7.7]	r CR (c/s) for	/s) for	CR (c/s) for L= $[5.5-7.7]$ CR (cts/s) for L= $[5.5-7.7]$:



Total Relativistic Electron Content (TREC)

To take into account the non-symmetric aspect of Earth's magnetic field the Total Relativistic Electron Content (TREC) is computed for the three Years (1995, 1996, 1997):

Count rate data is :

- Initially binned as a function of L by averaging in steps of ΔL = 0.2
- Then approximated by T(L)=C(L)×L², where the factor L² makes an allowance for the volume occupied between dipolar shells L and L+ΔL

(for more details see Iles R.H.A., Fazakerley A.N., Johnstone A.D., Meredith N.P. and Bühler P, Ann. Geophys., 20, 7, 957-965, 2002)

The TREC is computed as a function of day for the following three radiation belt intervals:

L=[4.1,5.5], L=[5.5,7.7] and L=[4.1,7.7]



U

aeronomie.b

OUTER ELECTRON RADIATION BELT

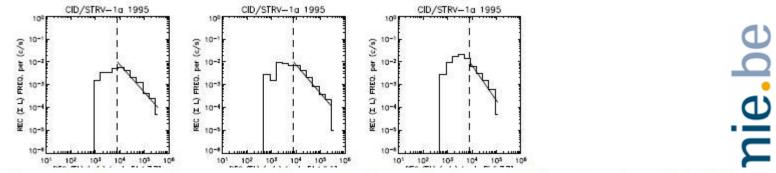
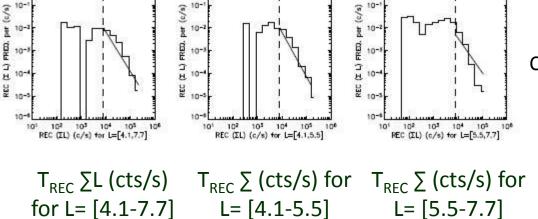


Table 3. Characteristics of the total relativistic electron content (T_{REC}) frequency distributions for different years and L-shell intervals.

Year	4.1–7.7 interval	4.1–7.7 slope	4.1–5.5 interval	4.1-5.5 slope	5.5–7.7 interval	5.5–7.7 slope
1995	[8000,359717]	-1.195 ± 0.060	[8000,274153]	-1.254 ± 0.069	[8000,111914]	-1.548 ± 0.122
1996	[8000,270400]	-1.535 ± 0.082	[8000,199090]	-1.430 ± 0.104	[8000,71309]	-2.074 ± 0.193
1997	[8000,216389]	-1.739 ± 0.092	[8000,160989]	-1.950 ± 0.119	[8000,109188]	-2.675 ± 0.234



Crosby N., Meredith N., Coates A., Iles R., NPG, 12, 993, 2005





EARTH'S OUTER ELECTRON RADIATION BELT SUMMARY

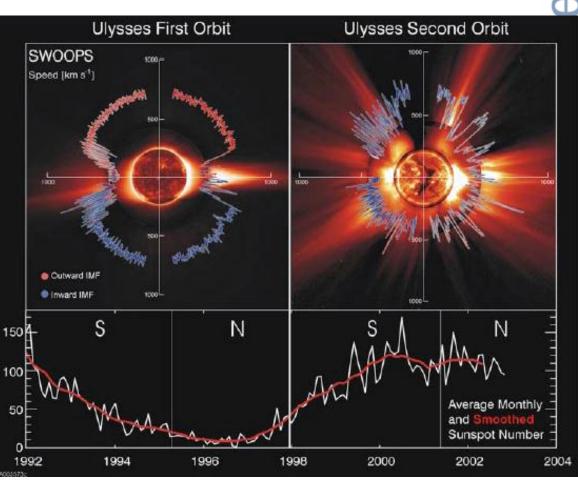
- Results suggest that the modelling of the outer electron radiation belt as a complex system in a self-organized critical state provides a good context to understand the frequency distributions of the electron parameters.
- Evidence for more dynamic control in the outer region of the outer
 electron radiation belt.
- Entire outer electron radiation belt appears to be affected in the same way.
- Any successful model should be able to explain [or at least to reproduce] the results of statistical studies performed on the data.

Solar Wind: The discovery of two regimes

Ulysses spacecraft measurements of the solar wind speed and IMF polarity in the 3-D heliosphere at times near:

- solar min. (top left-hand panel)
- solar max. (top right-hand panel).

Sunspot number as a function of time.



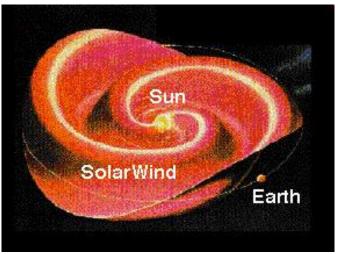
McComas et al. (2003)



υ aeronomie.b

Electron enhancements in the radiation belts are for the most part correlated with:

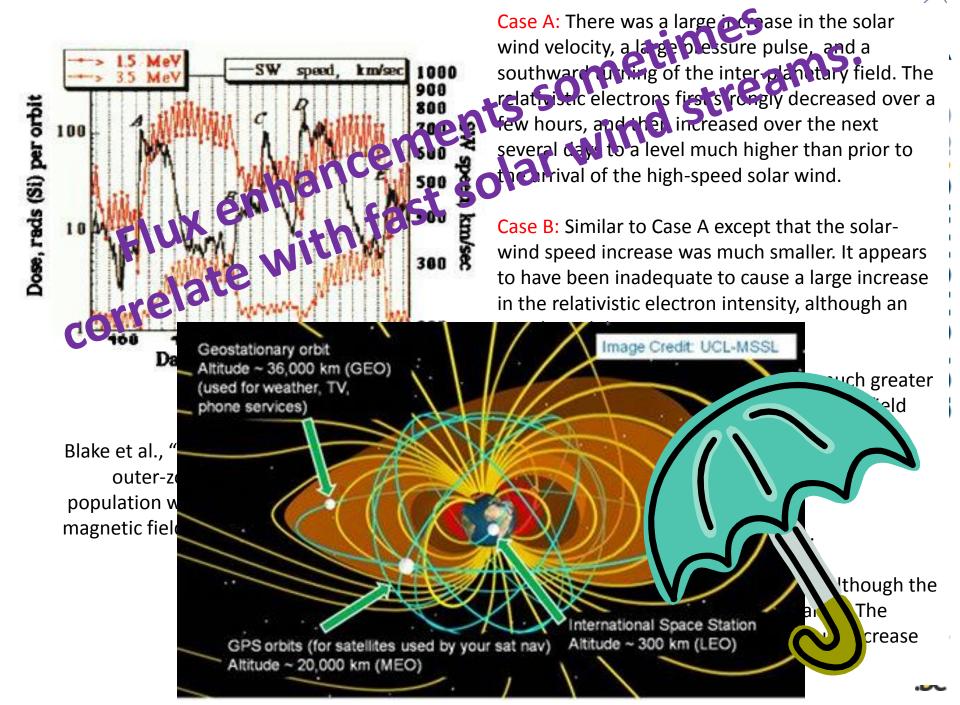
- Fast solar wind streams [Paulikas and Blake, 1979; Baker et al., 1986].
- CME events [Li et al., 1993].
- IMF Bz < 0 [Blake et al., 1997].
- Magnetic storms [Baker et al., 1986; Reeves, 1998].

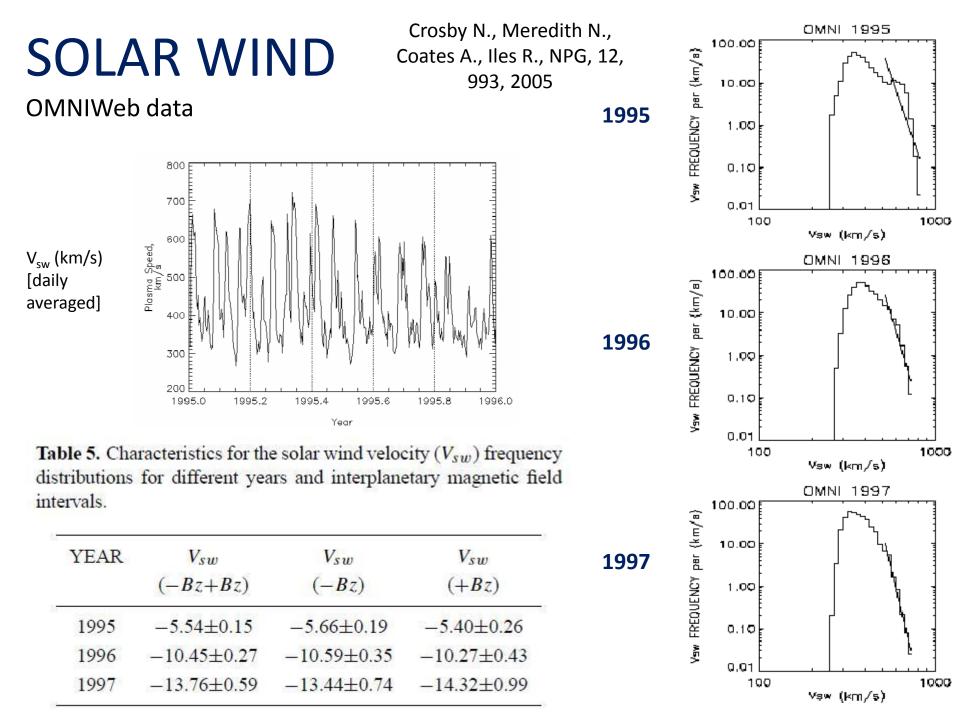


Vsw > 500 km/s Bz < 0 nT

L1 monitoring of the solar wind is vital for space weather forecasting!



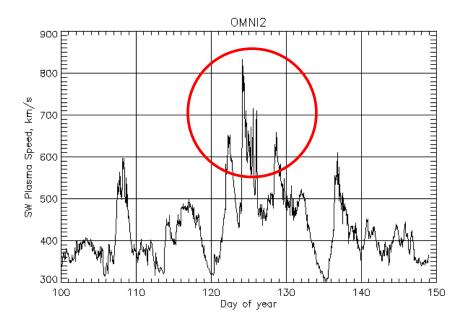




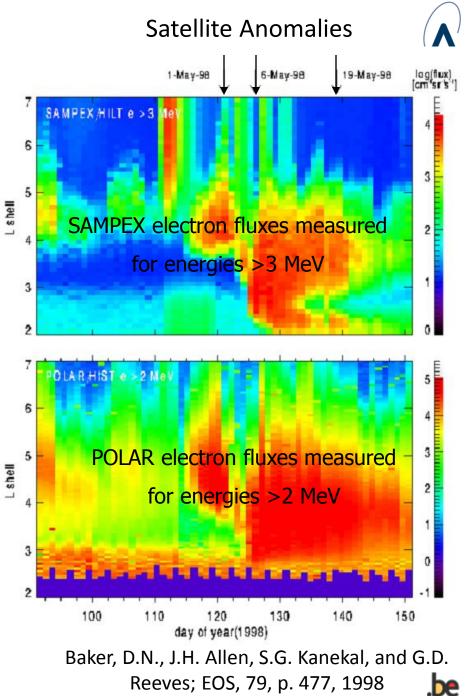


	Outer El	CID/STRV-1a ectron Radiation E	OMNI Solar Wind Data			
Year	T _{REC} (ΣL) 4.1 < L< 7.7 slope	TREC (ΣL) 4.1 < L< 5.5 Slope	TREC (ΣL) 5.5 < L < 7.7 slope	Vsw (-Bz & +Bz) slope	Vsw (-Bz) slope	NONO
1995	-1.195+/-0.060	-1.254+/-0.069	-1.548+/-0.122	-5.54+/-0.15	-5.66+/-0.19	APri
1996	-1.535+/-0.082	-1.430+/-0.104	-2.074+/-0.193	-10.45+/-0.27	-10.59+/-0.35	-
1997	-1.739+/-0.092	-1.950+/-0.119	-2.675+/-0.234	-13.76+/-0.59	-13.44+/-0.74	-

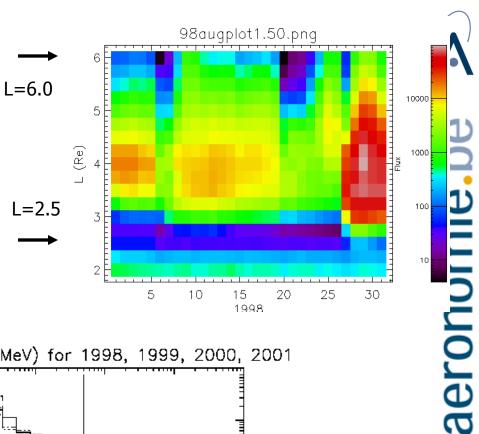
Crosby N., Meredith N., Coates A., Iles R., NPG, 12, 993, 2005

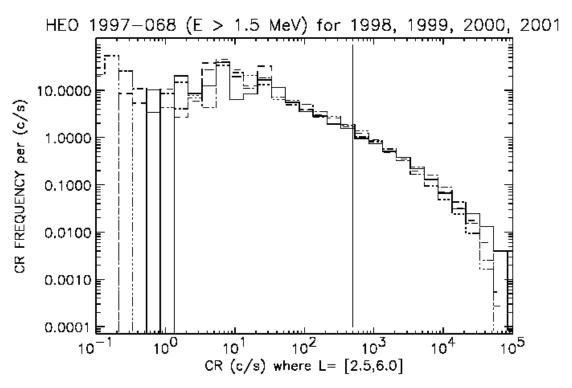


A very intense flux of electrons evident in the magnetosphere during May 1998 may have caused the Galaxy 4 satellite failure.



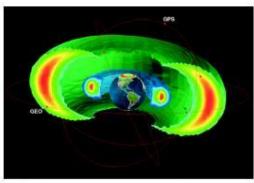
Daily Averaged Electron Outer Radiation Belt Count Rate Data HEO data courtesy of The Aerospace Corporation





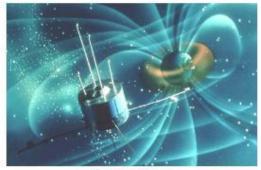






Credit: NASA/RBSP





Credit: ESA/BAS

The Earth's Radiation Belts: Physical Processes and Dynamic Modeling



aero



